Illuminating Glucomannan Synthases to Explore Cell Wall Synthesis Bottlenecks

Annika Grieß-Osowski, Madalen Robert, Moni Qiande, Stefanie Clauss, Cătălin Voiniciuc*

Corresponding Author:

Cătălin Voiniciuc – Horticultural Sciences Department, University of Florida, Gainesville, FL 32611, USA; https://orcid.org/0000-0001-9105-014X; Phone: +1 352-273-4782; Email: cvoiniciuc@ufl.edu

Abstract

Hemicelluloses are important dietary fibers and a key component of lignocellulosic biomass. Despite numerous observations for fluorescently tagged cellulose synthases, the subcellular journeys and biochemical activities of intracellular cellulose synthase-like enzymes such as β-mannan synthases (ManS) remain largely unexplored. This study identifies C-terminal fluorescent protein tags that maintain ManS activity in the yeast *Pichia pastoris* to accelerate the Design, Build, Test, Learn cycles for polysaccharide biosynthesis. Using the *Amorphophallus konjac* ManS as a case study, we demonstrate that the enzyme co-localizes with a known yeast marker for the Golgi apparatus despite the toxic effects of plant glucomannan accumulation in yeast. The ManS first transmembrane domain was found to be critical for the punctate localization of the enzyme, its overall expression level and its function. Additionally, we explored how fluorescently tagged ManS is influenced by genetic or chemical perturbations of native yeast cell wall components, such as reducing protein mannosylation and severe disrupting β-1,3-glucans. Finally, we tested alternative promoters and vector backbones for integrative or episomal ManS expression to address outstanding questions regarding hemicellulose production. We propose that expanding the Plant MoClo-compatible plasmid repertoire is essential to swiftly prototype carbohydrate-active enzymes in yeast before proceeding with more time-intensive analyses in plants. By shortening glycan experiments from weeks or months in bioenergy crops to mere hours or days, our yeast strategies provide insights on how to de-risk the biodesign of plant cell walls.

Keywords: plant cell wall, polysaccharides, cellulose synthase-like enzymes, hemicellulose, yeast bioengineering,

Introduction

Enzymes from the cellulose synthase (CESA) superfamily elongate cellulose and most hemicelluloses,[1] which collectively form the main network of fibers in plant cell walls. In the last two decades, N-terminal fluorescent protein (FP) tags on CESA proteins became popular tools to study cell wall dynamics and have revealed molecular insights into the localization and trafficking of CESA complexes *in planta.*[2–4] While FP-CESAs are only active once secreted to the plasma membrane, CESA-like (CSL) enzymes producing β-1,4-linked mannans (CSLA), xyloglucan (CSLC), or mixed-linkage glucans (CSLF, CSLH, and CSLJ) function predominantly in the Golgi apparatus and their products are delivered extracellularly.[5] However, the subcellular journeys and biochemical activities of most CSL enzymes have remained hidden, limiting long-standing aims to increase hexose sugar content (e.g. glucose, Glc, and mannose, Man) in bioenergy crops. For example, a prior attempt to boost mannan production in seeds through CSLA overexpression strategies not only failed to enhance cell wall composition,[6] but caused severe genetic and metabolic perturbations.

Since plant transformation remains slow compared to microbial bioengineering, surrogate hosts are needed to accelerate Design, Built, Test, Learn cycles for polysaccharide biosynthesis or modification.[7] Recently, *Pichia pastoris* (also known as *Komagataella phaffii*) has emerged as a promising yeast cell factory to study how plant CSLAs produce (gluco)mannans.[8] While classical *in vitro* assays require microsomal extracts and radiolabeled nucleotide sugar donors,[9,10] endogenous precursors in *Pichia* cells are sufficient for plant β-1,4-mannan and β-1,4-glucan synthases and their co-factors.[8,11,12] Nevertheless, the attachment of superfolder GFP (sfGFP) to the N-terminus of β-mannan synthases such as the *Amorphophallus konjac* AkCSLA3, referred to as ManS for the remainder of the article, significantly reduced or abolished activity in yeast. Here, we explore the influence of FPs at the C-terminal end of ManS and extend the portfolio of genetic and chemical tools available to investigate plant hemicellulose production in yeast cells.

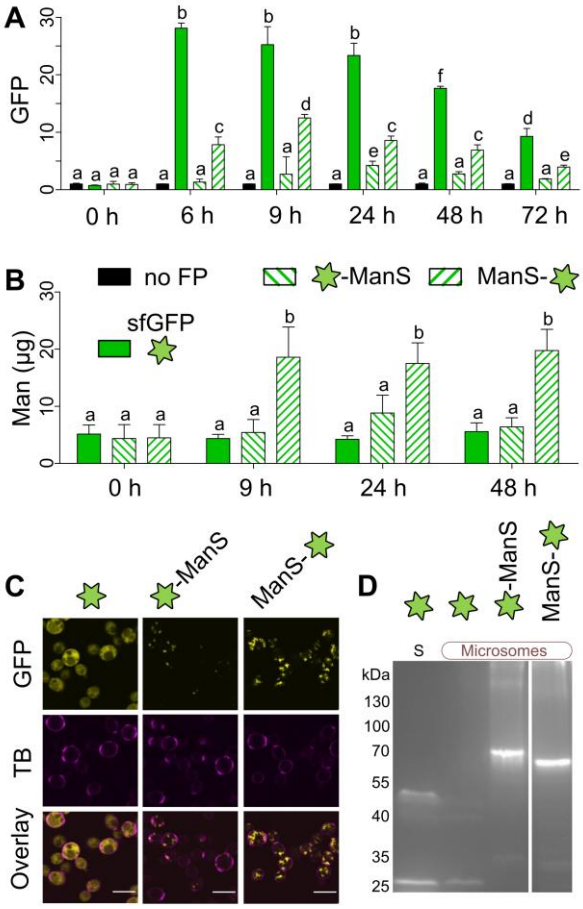

Figure 1: Expression of sfGFP tags in Pichia. Pre-cultured cells were induced using methanol. (A) Fold change in fluorescence relative to the empty vector control. (B) Man content of AKI polymers in equal aliquots at different timepoints. Data show mean + SD from three biological replicates. Letters denote significant changes (one-way ANOVA with Tukey test, $P < 0.05$). (C) Protein localization at 24 h post-induction. Cell walls were labelled with trypan blue (TB). Scale bars = 5 µm. (D) In-gel fluorescence of soluble (S) and microsomal proteins after electrophoresis in non-denaturing conditions.

Results and Discussion

Building A Set of Functional ManS-FP Fusions

First, we generated a ManS-sfGFP containing C-terminal tag in the pPICZ B vector, and compared it to the previously tested[8] sfGFP-ManS. Seeking to determine the importance of induction time, cells

were first grown in glycerol-containing medium for biomass accumulation. The sfGFP control strain and new ManS-sfGFP lines showed significant expression within 6 h of methanol induction and their relative fluorescence peaked within 9 h (Figure 1A). Consistent with the fluorescence data, ManS-sfGFP increased the Man content to ~20% of alkaline-insoluble (AKI) polymers after 9 h of induction, with no further increases at later timepoints (Figure 1B). In contrast, sfGFP-ManS required 24 h of induction to reach its maximal expression (still ≥2-fold lower than ManS-sfGFP) only reached ~10% Man. Therefore, C-terminal ManS tagged construct expressed well and provided a reliable proxy for the relative quantity of mannan made.

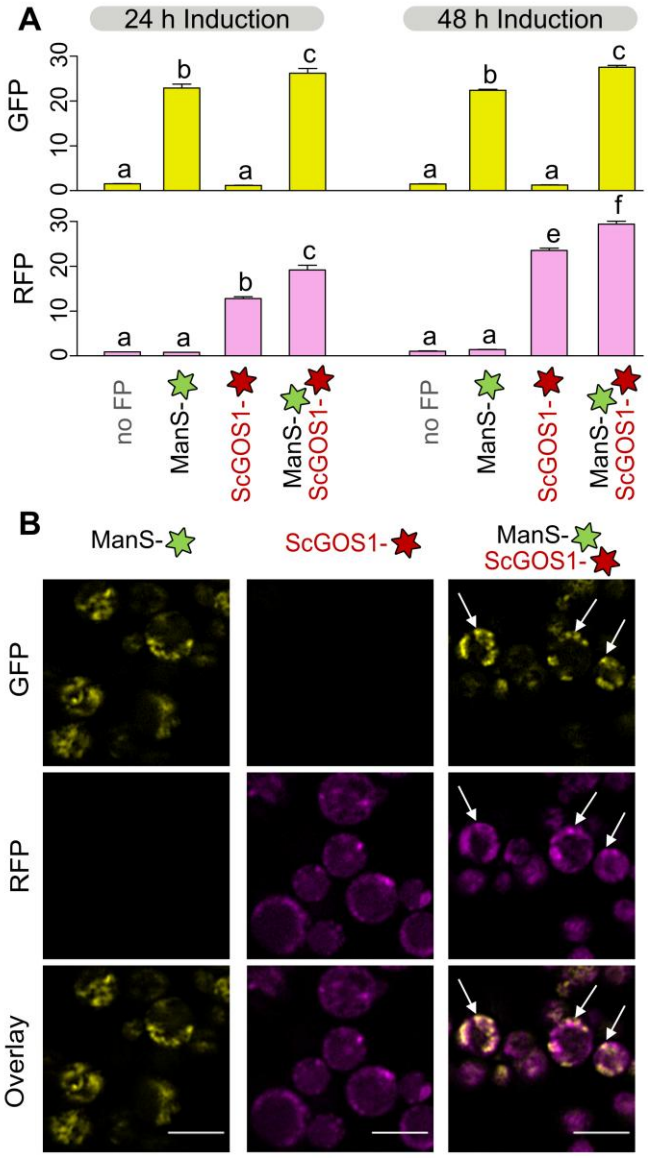

Figure 2. Co-localization of ManS with a Golgi marker. (A) Fold change of normalized GFP and RFP signal relative to no FP control post methanol induction. Data show the mean + SD of three biological replicates and different letters denote significant changes (one-way ANOVA with Tukey test, $p < 0.05$). (B) Arrows mark co-localized signals at 48 h. Scale bars = 5 µm.

Compared to the cytosolic distribution of free sfGFP (**Figure 1C**), tagged ManS localized in intracellular punctae, with brighter and a greater number of fluorescent bodies observed for the C-terminal sfGFP fusion. To ensure that the sfGFP remains attached to ManS, soluble and microsomal protein fractions were examined with in-gel fluorescence and non-denaturing conditions. On its own, sfGFP primarily showed the expected 27 kDa in the soluble fraction, with an additional ~50 kDa band representing dimers. Tagged ManS was detected in the microsomal fraction, just below the predicted ~87 kDa, with no signs of sfGFP cleavage or significant protein glycosylation. Therefore, the sfGFP-tagged ManS enzymes could be an enabling tool for future studies to decipher the detergent solubility, topology, and substrate specificities of CSL proteins.

In addition to sfGFP, which fluoresces regardless of its partner protein's folding status,[13] we found that Venus (a yellow FP that tolerates lower pH values) and mRuby2 (a monomeric red FP) express well in *Pichia* (**Figure S1**). However, the three FPs had different dynamic ranges for fluorescence intensity in yeast. In the pPICZ B vector, ManS-Venus had ~20x higher fluorescence compared to no FP control, followed by ManS-sfGFP (~5x), while ManS-mRuby2 fluorescence was barely detected (~1.25x). Despite this large variation, all ManS-FP constructs produced more Man-containing polymers than sfGFP-ManS (**Figure S1**) and the FP-only controls. Since ManS-sfGFP produced the most glucomannan of the tested combinations, we prioritized this construct for further experiments in this study.

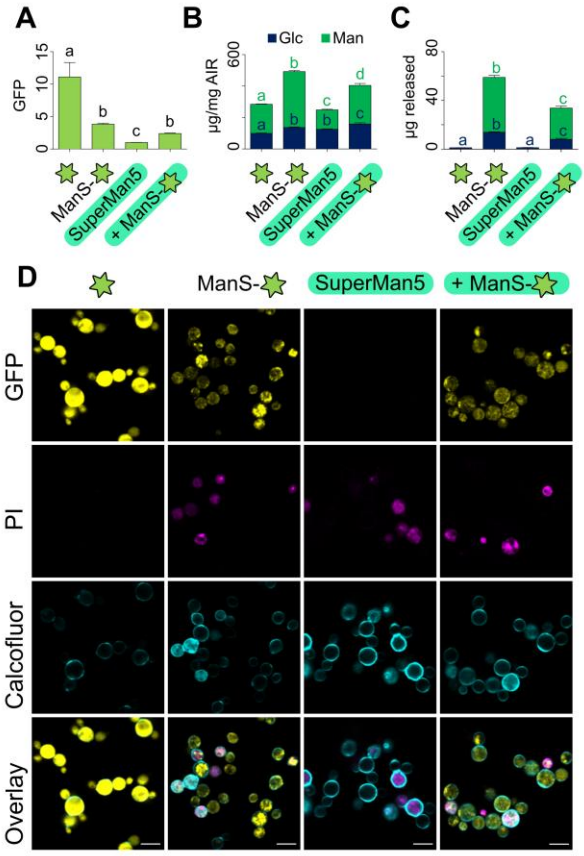

Figure 3. Glucomannan synthesis in the SuperMan5 strain after 48 h in YPM+G. (A) Fold change in GFP signal relative to SuperMan5 control. (B) Composition of total AIR and (C) solubilized carbohydrates after endo-β-mannanase treatment. Data show the mean + SD of six (A and B) or four (C) biological replicates. Different letters denote significant changes (one-way ANOVA with Tukey test, P < 0.05). (D) Confocal micrographs of cells stained with calcofluor white and PI before imaging. Scale bars = 5 µm.

Golgi Localization and Modification of the Metabolic Sink for GDP-Man

We hypothesized that ManS-sfGFP elongated β-mannan in the Golgi apparatus, which was previously visualized in *Pichia* using ScGOS1 as a reporter protein.[14] We assembled a ScGOS1-mRuby2 construct driven by the constitutive *pGAP*, and monitored co-expression with ManS-sfGFP after methanol induction (**Figure 2A**). Both ManS and ScGOS1 localized in overlapping punctae (**Figure 2B**), with similar distribution at all tested timepoints. However, ManS-sfGFP expression, localization and function could be severely impaired by deleting its first transmembrane domain (ΔTM1). The ΔTM1-ManS-sfGFP expressed poorly, aggregated in only one or a few larger subcellular compartments per cell, and did not produce mannan (**Figure S2**). The unexpected importance of TM1 for Golgi localization and protein folding or stability could explain lower activity of the N-terminal tagged ManS construct (**Figure 1**) and the malfunction of prior domain swaps in this CSLA protein region.[12]

To test whether β-mannan production in yeast is limited by competition for GDP-Man, we introduced ManS-sfGFP in the SuperMan5 commercial strain, which disrupts the *OCH1* α-1,6-mannosyltransferase required for yeast protein mannosylation.[15] ManS-sfGFP expressed slightly less (P > 0.05) in SuperMan5 but still showed a punctate localization (**Figure 3)**. Consistent with prior observations,[12] ManS expression was toxic to yeast and elevated propidium iodide (PI) uptake. Although SuperMan5 is reported to have normal doubling time,[15] we saw partial PI uptake in this glycoengineered strain even without ManS. In the alcohol-insoluble residue (AIR), encompassing all native yeast cell wall polymers, the SuperMan5 strain contained less Man than the X-33 wild-type (**Figure 3B**), but had a previously unreported increase of Glc that suggest an overproduction of yeast β-1,3-glucans. We hypothesized that the mutation of *OCH1* in SuperMan5 cells would free up GDP-Man for the synthesis of glucomannan. Although ManS-sfGFP expression raised hexose sugar content in the total AIR of both backgrounds compared to controls, the Man increase was not as high in SuperMan5 compared to X-33. We then isolated AKI polymers from this material and used an endo-β-mannanase to specifically solubilize and quantify plant glucomannan. SuperMan5 did not boost the activity of ManS, nor alter the 1 Glc to 3 Man ratio of its products (**Figure 3C**). These results indicate that factors other than GDP-sugar allocation are rate-limiting for ManS, since *OCH1* disruption did not promote the redistribution of Man units from yeast mannoproteins into

plant glucomannan. Indeed, ManS activity in the X-33 background was previously elevated by co-expression with plant Mannan Synthesis-Related (MSR) proteins that act as co-factors.[8]

Chemical Treatments of ManS-Expressing Cells

Using the fluorescent strains established in this study and known disruptors of cell wall glycans or their secretion, we evaluated how exogenous treatments modulate yeast growth, morphology, and polysaccharide biosynthesis. ManS-sfGFP expression and products were quantified in methanol-

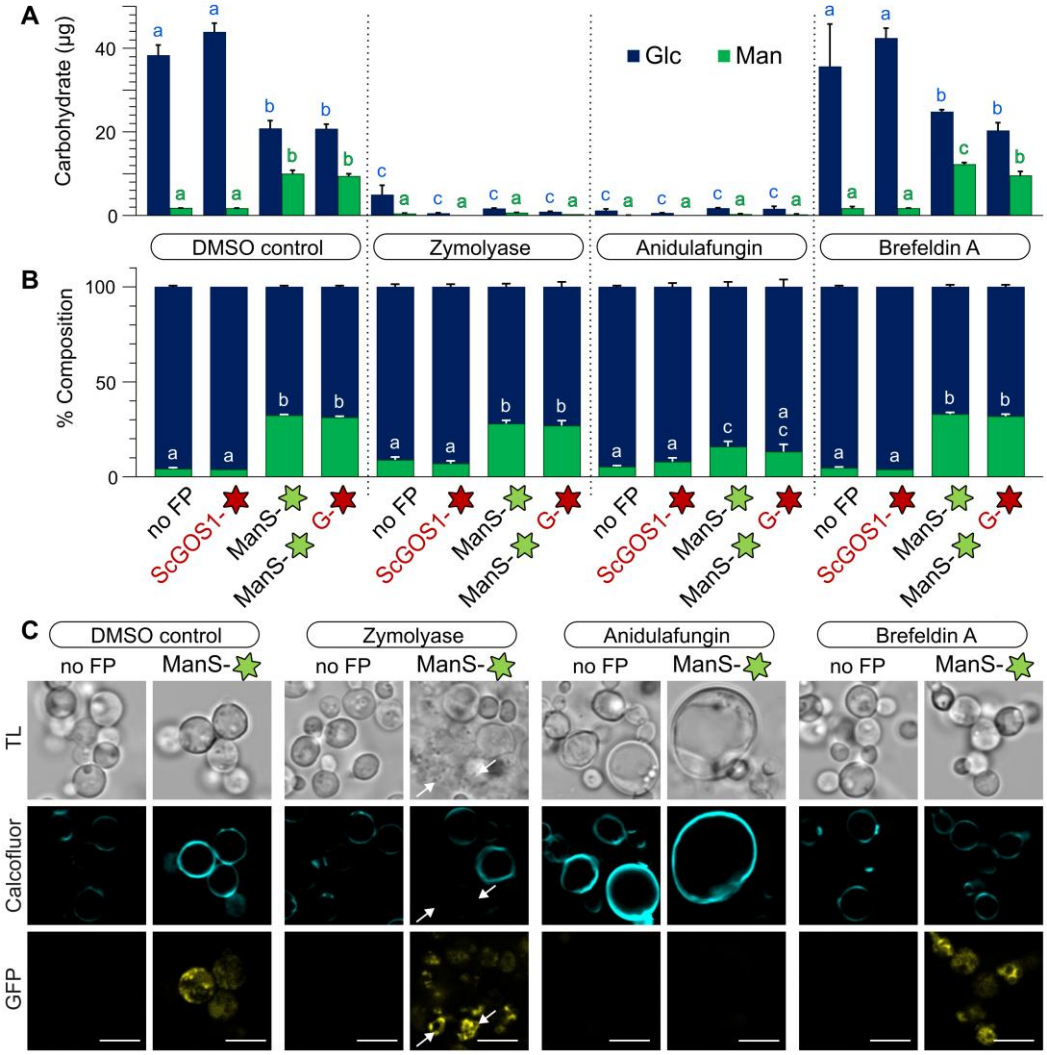

Figure 4. Modulating yeast wall composition and morphology using exogenous treatments. Cells pre-cultured in YPD were transferred for 48 h with YPM plus the indicated treatments. Absolute amounts (A) and relative composition (%, w/w) of AKI polymers (B). Error bars show mean + SD of three biological replicates. Letters denote significant differences obtained by one-way ANOVA with Tukey's pairwise ($P < 0.05$). (C) Confocal images of treated *Pichia* cells counterstained with calcofluor white. Similar GFP signals were observed with or without the expression of ScGOS1. Scale bar = 5 µm.

containing media supplemented with dimethyl sulfoxide (DMSO) only, Zymolyase 20T, Anidulafungin, or Brefeldin A (BFA). BFA, which induces intracellular aggregates in plants,[16] led to more diffuse ManS-sfGFP localization (**Figure 4C**), but still resembled the glycan profile of the DMSO control. With either DMSO or BFA, ManS-expressing strains accumulated more Man but less Glc than the empty vector and ScGOS1 Golgi marker alone, consistent with a growth penalty for glucomannan production (**Figure**

4A). Those changes pale in comparison to the Zymolyase and Anidulafungin treatments, which dramatically reduced yeast biomass and the insoluble polysaccharide content for all genotypes.

Zymolyase 20T directly hydrolyzes fungal β-1,3-glucans in the extracellular matrix, while Anidulafungin disrupts the same polymers via a distinct mode of action. As an antifungal drug that directly binds and inhibits glucan synthases with multiple TM domains,[17] Anidulafungin led to severe swelling (**Figure 4C**), increasing cell size by up to 3-fold compared to the DMSO control. Although ManS-sfGFP significantly increased the % Man of AKI in all four treatments (**Figure 4B**), Anidulafungin-treated cells were the least productive. The loss of sfGFP fluorescence in swollen Anidulafungin-treated cells could be due to severely impaired Golgi membrane integrity and/or ManS stability (**Figure 4C**). In contrast, *Pichia* cells with partly inactivated synthases were recently shown to have milder 17–28% reductions in β-1,3-glucans, but increased mannoprotein content and GFP expression.[18] Similar to our findings, the genetic impairment of glucans increased yeast cell size.[18] In contrast, the Zymolyase treatment did not alter the punctate ManS-sfGFP localization even in cells with lysed walls and reduced labeling with calcofluor white. The pharmacological results underscore the potential to redesign *Pichia* cell walls and to potentially displace fungal components with plant-based polymers. Our data indicate that extracellular digestion could be a superior strategy to preserve membrane integrity (**Figure 4B**).

Transcriptional Control of Hemicellulose Production in Yeast

Taking advantage of the functional ManS-sfGFP fusion protein, we evaluated which alternative promoters and vector backbones could speed up screens for hemicellulose production in *Pichia*. Using Golden Gate cloning and the GoldenPiCS kit,[19] previously used to assemble chimeric CSLA and CSLC enzymes,[12] we tested several promoters with the same transcriptional terminator for their ability to drive ManS-sfGFP fluorescence and mannan production (**Figure 5A, B**). While the constitutive *pGAP* worked best for the GFP control, none of the colonies genotyped as containing the pGAP-ManS showed any detectable fluorescence or β-mannan production. Therefore, constitutive ManS expression acts as a *de facto* negative selection marker, echoing the fitness penalty seen for direct methanol induction of *pAOX1:ManS-sfGFP* lines (**Figure 4A**).

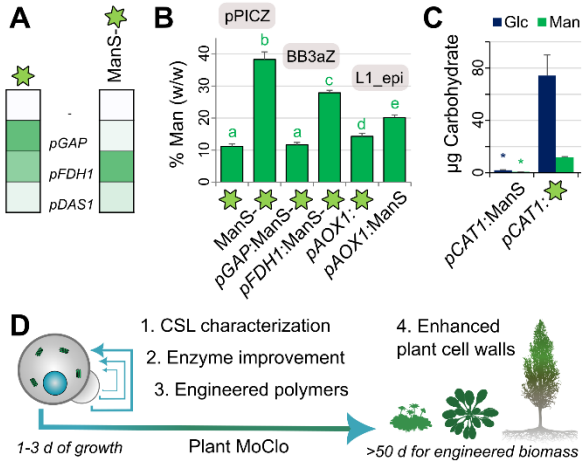

Figure 5. Promoters and episomal vectors to screen for plant cell wall synthases. (A) Heatmap of relative promoter activities for sfGFP versus ManS-sfGFP. (B) Man content of AKI polymers using three vector backbones with *pGAP* serving as a negative control. (C) Episomal expression with the *pCAT1* promoter leads to early induction and reduced biomass. (D) Proposed strategy to screen for CSL natural and engineered sequences in yeast, for later validation and application in plants.

We then built and tested episomal vectors for promising alternative for strong, inducible protein expression. The recently described *pPAP002* vector is compatible with the Plant MoClo kit,[20] which is versatile for experiments in plants. While episomal expression vectors require continuous selection pressure in culture media (typically antibiotics), they are easier to transform and bypass the need to purify linearized DNA for stable genome integration. We were initially surprised to find poor growth for *pPAP002* + *ManS* compared to *pPAP002* + *sfGFP* when co-feeding glycerol and methanol (**Figure 5C**). Since the methanol-inducible *pCAT1* promoter found in the *pPAP002* vector can be de-repressed by glucose or glycerol depletion,[21] we generated a new Plant MoClo L1 episomal vector that can accept any promoter and terminator. Using different carbon feeding regimens, we found that the episomal plasmid with *pCAT1* drove higher sfGFP expression than the

same backbone with *pAOX1* (**Figure S3**), the gold standard for *Pichia* expression, but led to a partial growth penalty. Therefore, we pivoted to express ManS using *pAOX1* in the MoClo L1 episomal vector and found a good compromise between mannan production (**Figure 5B**) and biomass accumulation. Although Man accumulation via episomal ManS expression was lower than the genomic integrations, the new Plant MoClo L1 vector provides higher transformation efficiency and more room for activity improvement to enable future screens of CSLA biodiversity or directed evolution campaigns.

Conclusions

Pichia cells provide a unicellular testbed for chromosomal transgene integrations or episomal DNA replication (**Figure 5D**) and accumulate enough carbohydrates for biochemical analyses in as little as 9 h post-induction (**Figure 1**). Fluorescently-tagged ManS enzymes are now available to answer a range of biological questions. For example, future studies could test hypotheses about CSLA topology around the Golgi membrane.[22] Although *in vitro* yeast experiments predicted a need for dedicated transporters to deliver GDP-sugars for CSLA activity in the Golgi lumen,[23] none of the canonical GDP-Man transporters were found to influence glucomannan synthesis in Arabidopsis plants,[24] and our results in the SuperMan5 strain suggests that glucomannan production was not limited by the *Pichia* nucleotide sugar pool. Furthermore, since the most popular yeast Golden Gate toolkits are not compatible with the Plant MoClo standard,[25] there is a clear need to expand the plasmids available quickly test and de-risk carbohydrate-active enzymes in yeast before assembling parts for more time-consuming steps in plants (**Figure 5D**). The strategies presented in this study, including the potential to genetically and chemically dose the biosynthesis of different glycans, underscore the value re-designing plant cell walls using yeast.

Methods

Vector construction and transformation

Table S1 summarizes the plasmids used in this study, the molecular cloning strategies. The pPICZ classical cloning and GoldenPiCS assembly into BB3aZ_14 [19] were previously described.[8,12] Unless otherwise indicated, all ManS constructs were driven by the methanol-inducible *pAOX1*, integrated into the *AOX1* genomic region, and selected using Zeocin. New parts were amplified with the High-Fidelity Phusion DNA Polymerase (Thermo Fisher Scientific, Cat# F530L) and the primers listed in **Table S2**. The BB3rN_14 backbone[19] was used for the pGAP:ScGOS1 expression and Nourseothricin selection. The pPAP002 vector[20] was modified using NEBuilder HiFi DNA Assembly Cloning Kit (New England Biolabs) to yield a *Pichia* episomal expression L1_2F_ePH vector that can accept any Promoter-Gene-Terminator combination following the Plant MoClo syntax[26]. After sequence-verification of new parts, linearized plasmids (for genome integration) and circular episomal constructs were transformed into *Pichia* via electroporation,[27] and at least three PCR-verified independent were screened.

Pichia growth and medium composition

Cells were cultivated in an Eppendorf Innova 42R at 30°C and 250 rpm in 24-well plates, for 48 h unless otherwise specified. Most batches were grown in YP base medium containing 1% (w/v) yeast extract, 2% (w/v) peptone was supplemented with 2.0% (w/v) dextrose/glucose for YPD; or 1.5% (v/v) methanol for YPM, or in YP containing more than one carbon source as specified in the figure legends. For **Figure S1** (A and B), buffered media were prepared according to the EasySelect *Pichia* Expression Kit (ThermoFisher Scientific). For episomal vectors, the liquid media was supplemented with hygromycin (150 µg/mL) to ensure the plasmids are retained.

For biomass accumulation, cells were pre-cultured in ≥2 mL of glycerol-rich medium for at least 24 h followed by centrifugation at 2000 g for 2 min, and resuspension in a similar volume of methanol-containing medium for 24–72 h of induction. For the antifungal treatments, 2 mg of Zymolyase 20T (Carl Roth, Cat# 9324.3), 6 µg of Anidulafungin (Sigma Aldrich, Cat# SML2288-5MG), or 8 µg of Brefeldin A (VWR International GmbH, Cat# CAYM11861-10) dissolved in DMSO were applied per mL of *Pichia* culture.

To isolate sufficient protein for in-gel fluorescence, we cultivated yeast for 24 h in 50 mL of YPD from an initial OD600 of 0.3, followed by centrifugation (5 min at 2000 *g*), resuspension, and growth in 50 mL of YPM for another 24 h.

Plate reader measurements and in-gel fluorescence

For plate reader assays, equal aliquots of cell suspensions were diluted with water to avoid saturation and analyzed in 96-well plates. OD600 and fluorescence (excitation/emission peaks: 485/511 for GFP, 513/527 nm for Venus, and 569/593 nm for mRuby2) were measured using Tecan M1000 (Grödig, AT) or BioTek Synergy H1 plate reader (Agilent Technologies, USA) plate readers. We compared relative fluorescent units (normalized to OD600) or fold changes relative to cells without FPs.

Microsomal proteins were extracted from *Pichia* cultures based on a prior method,[28] with slight modifications, starting with a cell lysis containing 50 mM Tris-HCl (pH 7.6), 150 mM NaCl, and 1x Pierce protease inhibitors (Thermo Fisher, Cat# A32955). *Pichia* cells were milled with glass beads in a Retsch MM400 homogenizer for a total of 7 cycles, each consisting of 3 min at 20 Hz for 3 min, followed by cooling on ice. After centrifugation at 3000 *g* and 4°C for 20 min, the supernatant was transferred to new tubes and centrifuged at 20000 *g* for 1 h at 4°C to separate the microsomal membrane and soluble cytosolic fractions. Following a Bradford assay,[29] 20 µg of proteins were diluted 1:5 with 5x Laemmli protein buffer and incubated for 5 min at 55°C. Samples were loaded alongside 2 µL of PageRuler ladder (Thermo Scientific) into a Mini PROTEAN Tetra cell (Bio-Rad, Hercules, US) with 1.0 mm thick gels, for electrophoresis in 1x ROTIPHORESE SDS-PAGE buffer (Carl Roth) at 100–150 V for 2 h. Protein were visualized (blue LED light plus GFP filter) in a UVP GelStudio PLUS Touch (Analytik Jena GmbH, DE).

Confocal microscopy

In general, cells were stained with 0.01% (w/v) of the specified dye immediately before imaging. Zeiss LSM880 micrographs (**Figures 1 and 3**) were acquired using a 40x/1.2 water-immersion objective, a beam splitter MBS 488/561 and AiryScan mode. The excitation/emission peaks were 488/523 nm for Venus, 561/579 nm for mRuby2 and TB. In the remaining micrographs, Zeiss LSM900 images were acquired using a 63x/1.20 water-immersion objective with AiryScan mode and the following excitation/emission parameters: CF (405/410–490 nm, SP545), Venus (488 nm/490–560 nm), PI (639 nm, 656–700 nm, LP655). For each panel, images were uniformly processed with ImageJ.[30]

Yeast cell wall analyses

Pichia cells were lysed, washed, and dried to obtain cell wall AIR or to directly enrich glucomannan AKI polymers as previously described.[8] For monosaccharide analyses, 50 µL aliquots of the AKI polymers suspension or 300 µg of dried AIR material were used for acid hydrolysis. Glc and Man were separated and quantified using high-performance anion-exchange chromatography coupled with pulsed electrochemical detection (HPAEC-PAD). The HPEAC-PAD setup applied a previously described 30 min eluent gradient[12] on a Metrohm 940 Professional IC Vario system equipped with a Metrosep Carb 2–250/4.0 column.

Abbreviations

ManS, β-mannan synthase

AKI, alkaline-insoluble polysaccharides

Author Information

Annika Grieß-Osowski – Independent Junior Research Group–Designer Glycans, Leibniz Institute of Plant Biochemistry, 06120 Halle (Saale), Germany

Madalen Robert – Independent Junior Research Group–Designer Glycans, Leibniz Institute of Plant Biochemistry, 06120 Halle (Saale), Germany

Moni Qiande – Horticultural Sciences Department, University of Florida, Gainesville, FL 32611, USA

Stefanie Clauss – Independent Junior Research Group–Designer Glycans, Leibniz Institute of Plant Biochemistry, 06120 Halle (Saale), Germany

Cătălin Voiniciuc – Horticultural Sciences Department, University of Florida, Gainesville, FL 32611, USA; Independent Junior Research Group–Designer Glycans, Leibniz Institute of Plant Biochemistry, 06120 Halle (Saale), Germany

Author Contributions: C.V. designed the experiments and A.G.-O., M.R. M.Q. and S.C. collected and analyzed data. C.V. prepared and revised the manuscript using draft text and figures from all authors.

Conflicts of Interest: The authors declare no competing financial interest.

Acknowledgments

C.V. gratefully acknowledges UF/IFAS startup funding, and the USDA National Institute of Food and Agriculture, Research Capacity Fund (Hatch) project 7004470, the UF Horticultural Sciences department. This work was also in part supported by the Deutsche Forschungsgemeinschaft (DFG;German Research Foundation grant no. 414353267 to C.V.) and by core funding (Leibniz Association) from the Federal Republic of Germany and the state of Saxony-Anhalt. The GoldenPiCS Kit (Addgene kit #1000000133) was a gift from the Gasser/Mattanovich/Sauer group. The MoClo Toolkit (Addgene kit # 1000000044)" and pPAP002 (Addgene plasmid #153489) were a gift from the Sylvestre Marillonnet Lab.

References

(1) Little, A.; Schwerdt, J. G.; Shirley, N. J.; Khor, S. F.; Neumann, K.; O'Donovan, L. A.; Lahnstein, J.; Collins, H. M.; Henderson, M.; Fincher, G. B.; Burton, R. A. Revised Phylogeny of the Cellulose Synthase Gene Superfamily: Insights into Cell Wall Evolution. *Plant Physiol.* **2018**, *177* (3), 1124–1141. https://doi.org/10.1104/pp.17.01718.

(2) Voiniciuc, C.; Pauly, M.; Usadel, B. Monitoring Polysaccharide Dynamics in the Plant Cell Wall. *Plant Physiology* **2018**, *176* (4), 2590–2600. https://doi.org/10.1104/pp.17.01776.

(3) DeVree, B. T.; Steiner, L. M.; Głazowska, S.; Ruhnow, F.; Herburger, K.; Persson, S.; Mravec, J. Current and Future Advances in Fluorescence-Based Visualization of Plant Cell Wall Components and Cell Wall Biosynthetic Machineries. *Biotechnology for Biofuels* **2021**, *14* (1), 78. https://doi.org/10.1186/s13068-021-01922-0.

(4) Polko, J. K.; Barnes, W. J.; Voiniciuc, C.; Doctor, S.; Steinwand, B.; Hill, J. L.; Tien, M.; Pauly, M.; Anderson, C. T.; Kieber, J. J. SHOU4 Proteins Regulate Trafficking of Cellulose Synthase Complexes to the Plasma Membrane. *Current Biology* **2018**, *28* (19), 3174-3182.e6. https://doi.org/10.1016/j.cub.2018.07.076.

(5) Zhang, B.; Gao, Y.; Zhang, L.; Zhou, Y. The Plant Cell Wall: Biosynthesis, Construction, and Functions. *J. Integr. Plant Biol* **2021**, *63* (n/a), 251–272. https://doi.org/10.1111/jipb.13055.

(6) Naoumkina, M.; Vaghchhipawala, S.; Tang, Y.; Ben, Y.; Powell, R. J.; Dixon, R. A. Metabolic and Genetic Perturbations Accompany the Modification of Galactomannan in Seeds of Medicago Truncatula Expressing Mannan Synthase from Guar (Cyamopsis Tetragonoloba L.). *Plant Biotechnology Journal* **2008**, *6* (6), 619–631. https://doi.org/10.1111/j.1467-7652.2008.00345.x.

(7) Pauly, M.; Gawenda, N.; Wagner, C.; Fischbach, P.; Ramírez, V.; Axmann, I. M.; Voiniciuc, C. The Suitability of Orthogonal Hosts to Study Plant Cell Wall Biosynthesis. *Plants* **2019**, *8* (11), 516. https://doi.org/10.3390/plants8110516.

(8) Voiniciuc, C.; Dama, M.; Gawenda, N.; Stritt, F.; Pauly, M. Mechanistic Insights from Plant Heteromannan Synthesis in Yeast. *Proc Natl Acad Sci USA* **2019**, *116* (2), 522–527. https://doi.org/10.1073/pnas.1814003116.

(9) Liepman, A. H.; Wilkerson, C. G.; Keegstra, K. Expression of Cellulose Synthase-like (Csl) Genes in Insect Cells Reveals That CslA Family Members Encode Mannan Synthases. *Proc. Natl. Acad. Sci. USA* **2005**, *102* (6), 2221–2226. https://doi.org/10.1073/pnas.0409179102.

(10) Gille, S.; Cheng, K.; Skinner, M. E.; Liepman, A. H.; Wilkerson, C. G.; Pauly, M. Deep Sequencing of Voodoo Lily (Amorphophallus Konjac): An Approach to Identify Relevant Genes Involved in the Synthesis of the Hemicellulose Glucomannan. *Planta* **2011**, *234* (3), 515–526. https://doi.org/10.1007/s00425-011-1422-z.

(11) Cocuron, J.-C.; Lerouxel, O.; Drakakaki, G.; Alonso, A. P.; Liepman, A. H.; Keegstra, K.; Raikhel, N.; Wilkerson, C. G. A Gene from the Cellulose Synthase-like C Family Encodes a β-1,4 Glucan Synthase. *Proc. Natl. Acad. Sci. USA* **2007**, *104* (20), 8550–8555. https://doi.org/10.1073/pnas.0703133104.

(12) Robert, M.; Waldhauer, J.; Stritt, F.; Yang, B.; Pauly, M.; Voiniciuc, C. Modular Biosynthesis of Plant Hemicellulose and Its Impact on Yeast Cells. *Biotechnol Biofuels* **2021**, *14* (1), 140. https://doi.org/10.1186/s13068-021-01985-z.

(13) Pédelacq, J. D.; Cabantous, S.; Tran, T.; Terwilliger, T. C.; Waldo, G. S. Engineering and Characterization of a Superfolder Green Fluorescent Protein. *Nature Biotechnology* **2006**, *24* (1), 79–88. https://doi.org/10.1038/nbt1172.

(14) Bevis, B. J.; Hammond, A. T.; Reinke, C. A.; Glick, B. S. De Novo Formation of Transitional ER Sites and Golgi Structures in Pichia Pastoris. *Nat Cell Biol* **2002**, *4* (10), 750–756. https://doi.org/10.1038/ncb852.

(15) Jacobs, P. P.; Geysens, S.; Vervecken, W.; Contreras, R.; Callewaert, N. Engineering Complex-Type N-Glycosylation in Pichia Pastoris Using GlycoSwitch Technology. *Nature protocols* **2009**, *4* (1), 58–70. https://doi.org/10.1038/nprot.2008.213.

(16) Voiniciuc, C.; Schmidt, M. H.-W.; Berger, A.; Yang, B.; Ebert, B.; Scheller, H. V.; North, H. M.; Usadel, B.; Günl, M. MUCILAGE-RELATED10 Produces Galactoglucomannan That Maintains Pectin and Cellulose Architecture in Arabidopsis Seed Mucilage. *Plant Physiology* **2015**, *169* (1), 403–420. https://doi.org/10.1104/pp.15.00851.

(17) Jospe-Kaufman, M.; Ben-Zeev, E.; Mottola, A.; Dukhovny, A.; Berman, J.; Carmeli, S.; Fridman, M. Reshaping Echinocandin Antifungal Drugs To Circumvent Glucan Synthase Point-Mutation-Mediated Resistance. *Angewandte Chemie* **2024**, *136* (9), e202314728. https://doi.org/10.1002/ange.202314728.

(18) Cheng, B.; Yu, K.; Weng, X.; Liu, Z.; Huang, X.; Jiang, Y.; Zhang, S.; Wu, S.; Wang, X.; Hu, X. Impact of Cell Wall Polysaccharide Modifications on the Performance of Pichia Pastoris: Novel Mutants with Enhanced Fitness and Functionality for Bioproduction Applications. *Microbial Cell Factories* **2024**, *23* (1), 55. https://doi.org/10.1186/s12934-024-02333-0.

(19) Prielhofer, R.; Barrero, J. J.; Steuer, S.; Gassler, T.; Zahrl, R.; Baumann, K.; Sauer, M.; Mattanovich, D.; Gasser, B.; Marx, H. GoldenPiCS: A Golden Gate-Derived Modular Cloning System for Applied Synthetic Biology in the Yeast Pichia Pastoris. *BMC Systems Biology* **2017**, *11* (1), 123. https://doi.org/10.1186/s12918-017-0492-3.

(20) Püllmann, P.; Knorrscheidt, A.; Münch, J.; Palme, P. R.; Hoehenwarter, W.; Marillonnet, S.; Alcalde, M.; Westermann, B.; Weissenborn, M. J. A Modular Two Yeast Species Secretion System for the Production and Preparative Application of Unspecific Peroxygenases. *Commun Biol* **2021**, *4* (1), 1–20. https://doi.org/10.1038/s42003-021-02076-3.

(21) Vogl, T.; Sturmberger, L.; Kickenweiz, T.; Wasmayer, R.; Schmid, C.; Hatzl, A.-M.; Gerstmann, M. A.; Pitzer, J.; Wagner, M.; Thallinger, G. G.; Geier, M.; Glieder, A. A Toolbox of Diverse Promoters Related to Methanol Utilization: Functionally Verified Parts for Heterologous Pathway Expression in Pichia Pastoris. *ACS Synth. Biol.* **2016**, *5* (2), 172–186. https://doi.org/10.1021/acssynbio.5b00199.

(22) Voiniciuc, C. Modern Mannan: A Hemicellulose's Journey. *New Phytologist* **2022**, *234* (4), 1175–1184. https://doi.org/10.1111/nph.18091.

(23) Davis, J.; Brandizzi, F.; Liepman, A. H.; Keegstra, K. Arabidopsis Mannan Synthase CSLA9 and Glucan Synthase CSLC4 Have Opposite Orientations in the Golgi Membrane. *The Plant Journal* **2010**, *64* (6), 1028–1037. https://doi.org/10.1111/j.1365-313X.2010.04392.x.

(24) Jing, B.; Ishikawa, T.; Soltis, N.; Inada, N.; Liang, Y.; Murawska, G.; Fang, L.; Andeberhan, F.; Pidatala, R.; Yu, X.; Baidoo, E.; Kawai-Yamada, M.; Loque, D.; Kliebenstein, D. J.; Dupree, P.; Mortimer, J. C. The Arabidopsis Thaliana Nucleotide Sugar Transporter GONST2 Is a Functional Homolog of GONST1. *Plant Direct* **2021**, *5* (3), e00309. https://doi.org/10.1002/pld3.309.

(25) Bird, J. E.; Marles-Wright, J.; Giachino, A. A User's Guide to Golden Gate Cloning Methods and Standards. *ACS Synth. Biol.* **2022**, acssynbio.2c00355. https://doi.org/10.1021/acssynbio.2c00355.

(26) Engler, C.; Youles, M.; Gruetzner, R.; Ehnert, T.-M.; Werner, S.; Jones, J. D. G.; Patron, N. J.; Marillonnet, S. A Golden Gate Modular Cloning Toolbox for Plants. *ACS Synthetic Biology* **2014**, *3* (11), 839–843. https://doi.org/10.1021/sb4001504.

(27) Lin-Cereghino, J.; Wong, W. W.; Xiong, S.; Giang, W.; Luong, L. T.; Vu, J.; Johnson, S. D.; Lin-Cereghino, G. P. Condensed Protocol for Competent Cell Preparation and Transformation of the Methylotrophic Yeast Pichia Pastoris. *Biotechniques* **2005**, *38* (1), 44, 46, 48. https://doi.org/10.2144/05381BM04.

(28) Drew, D.; Newstead, S.; Sonoda, Y.; Kim, H.; von Heijne, G.; Iwata, S. GFP-Based Optimization Scheme for the Overexpression and Purification of Eukaryotic Membrane Proteins in Saccharomyces Cerevisiae. *Nat Protoc* **2008**, *3* (5), 784–798. https://doi.org/10.1038/nprot.2008.44.

(29) Fanglian, H. Bradford Protein Assay Fanglian He. *Bio-protocol* **2011**, *1*, 4–5. https://doi.org/10.21769/BioProtoc.45.

(30) Abramoff, M. D.; Magalhaes, P. J.; Ram, S. J. Image Processing with ImageJ. *Biophotonics Int* **2004**, *11* (7), 36–42.

Supporting Information

Figure S1. *Pichia* expressing ManS with or without C-terminal FPs.

Figure S2. Impact of TM1 on ManS-sfGFP expression and activity.

Figure S3. Feed strategies and promoter performance for episomal vectors.

Table S1. Yeast vectors and strains used or constructed in this study.

Table S2. Primers used for cloning and genotyping in this study.
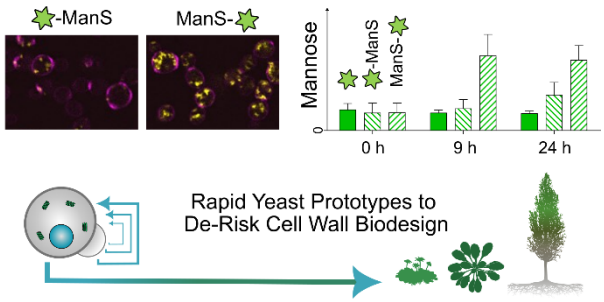
Graphical Abstract